A Novel Fast-EIS Measuring Method And Implementation for Lithium-ion Batteries

Pengfei Lu, Ming Li, Liqiang Zhang, Liqin Zhou
Department of Automation and Measurement, College of Engineering
Ocean University of China
Qingdao 266100, China
ZLQ @ ouc.edu.cn

***Abstract*—Energy store batteries play very important roles in the marine energy power station. Monitoring batteries' state for PHM study is necessary. Electrochemical Impedance Spectroscopy (EIS) is commonly used in battery state monitor. It can acquire detailed health features of batteries. This paper purposes a Fast-EIS measuring method, including the hardware design and frequency-mixing measuring algorithm based on the Fast Fourier Transformation (FFT). It can measure the EIS with a frequency range from 0.01Hz to 10kHz, and reduce 2/3 of the measuring time compared to the commercial electrochemical workstation, with enough accuracy. This method is suitable for implementation and engineering applications.**

Keywords- Lithium-ion battery; Fast-EIS; FFT; hardware implementation; LabVIEW

I. INTRODUCTION

Marine energy is an important part of sustainable energy. Compared with wind power and solar power, marine energy is randomness and instability, so a DC energy storage system is necessary to balance the power before inverting to the grid. The health state of energy store batteries will influence the security, reliability, and economy of the whole power station directly. So, monitoring the batteries' health state is necessary to keep the system operates properly and find the problem before failure. In existing methods, the Electrochemical Impedance Spectroscopy (EIS) is suitable for monitoring energy store batteries' internal health state. And it can describe the detailed health information rapidly without destroying the batteries [1].

The EIS data have already used in SEI-layer parameter [2], equivalent circuit modeling [3], and the effects of the loss of active material during aging for Lithium-ion batteries [4]. However, the measuring instruments used in those literatures are all commercial electrochemical workstations. And most of those are three-electrode structure. The wire resistance, the parasitic capacitance and parasitic inductance on the connector are existing, which may bring the measuring error. Commercial electrochemical workstations widely use the frequency-sweep method, which can only measure a single frequency point at a time, and the measuring speed is prolonged. Assuming that the frequency range is 0.01 Hz-10 kHz, and 10 points are taken per decuple frequency in the measuring process, there are 61 points to be measured. The total measuring time is about 1500 seconds when three periods are performed at each frequency point. Therefore, this method is usually used in laboratory research, and difficult to implement in the engineering field. What is worse, the battery's state may have changed during the long-time measuring process, affecting the measuring results of the EIS [5].

This paper aims at the EIS fast measuring by proposing a measuring instrument using NI Data Acquisition Card instead of commercial electrochemical workstation, and the EIS fast measuring method based on FFT. The remainder of this paper is organized as follows: Section II proposes the fast measuring algorithm, Section III provides the hardware design and verification, in Section IV two real Lithium-ion batteries are tested by the proposed method, and conclusions are drawn in the final section.

II. FAST-EIS ALGORITHM

A. Principle of the Fast-EIS

The Fast-EIS is based on the theory of FFT. Several sinusoidal signals of different frequencies are superposed and input to the electrochemical system in the meantime. If ten frequency points per decuple frequency are taken, there are 61 frequency points from 0.01Hz to 10kHz. And it's impossible to superpose those 61 points at the same time because the range of frequency is too wide. So, six frequency ranges are divided: 0.01Hz~0.1Hz, 0.1Hz~1Hz, 1Hz~10Hz, 10Hz~100Hz, 100Hz~1kHz, 1kHz~10kHz. The signals are superimposed in the six ranges separately. Taking 0.01Hz~0.1Hz for example, ten frequency points are extracted to generate a sinusoidal current signal and superimposed to a mixing-frequency current signal. Then the current signal is input to the battery should be:

$$y_I(t) = I_0 + \sum_{n=1}^{10} I_n \sin(2\pi f_n t + \phi_{I_n}) + N_I(t) \qquad (1)$$

where I_0 is the DC offset due to a certain deviation between the truth-value of the components such as the resistances in hardware circuit and the theoretical value, I_0 is small and can be ignored when the precision of the selected hardware components is high. I_n is the amplitude of different frequency current signal. f_n is the frequency point, $2\pi f_n$ is angular

978-1-7281-0860-5/19/$31.00 ©2019 IEEE

frequency. ϕ_{I_n} is the initial phase corresponding to the current signal at different frequencies. $N_I(t)$ is the measurement noise, which also small.

At the same time, the battery voltage response signal can be measured as:

$$y_V(t) = V_0 + \sum_{n=1}^{10} V_n \sin(2\pi f_n t + \phi_{V_n}) + N_V(t) \quad (2)$$

where V_0 is the battery's open-circuit voltage (OCV), this voltage can be compensated in hardware. V_n is the amplitude of different frequency voltage signal. fn is the frequency point, $2\pi f_n$ is angular frequency. ϕ_{V_n} is the initial phase. $N_V(t)$ is the measurement noise.

In this paper, the modified Hanning window is combined with the optimization theory to improve the FFT algorithm [6,7]. And the calculating accuracy of amplitude and phase is improved. The principle of the method is shown in Fig. 1.

The signals $y_I(t)$ and $y_V(t)$ in the time domain represented by (1) and (2) are respectively multiplied by a modified Hanning window [8], it can suppress spectrum leakage caused by signal truncation. Then the processed signal is calculated by the modified FFT. Using the signals close to f_n, the optimized spectrum information $Y_I(\omega)$ and $Y_V(\omega)$ can be obtained [9], and (3) is used to calculate the impedance at different angular frequencies. EIS curve can be drawn with the real part and the imaginary part of the impedance $Z(\omega)$.

$$Z(\omega) = \frac{Y_V(\omega)}{Y_I(\omega)} \quad (3)$$

B. Verification of the Fast-EIS

A mixing-frequency signal is generated using the frequency, amplitude and phase values in the corresponding columns of Table I. The traditional FFT algorithm (FFT toolbox in MATLAB) and the proposed algorithm is used to extract the signal information in every frequency. The Amplitude' and Phase' columns are the extracted results by traditional FFT, the Amplitude'' and Phase'' columns show the results by Fast-EIS method.

The relative errors of the two methods can be calculated as:

$$\Delta Amplitude1 = \frac{Amplitude' - Amplitude}{Amplitude} \times 100\% \quad (4)$$

$$\Delta Phase1 = \frac{Phase' - Phase}{Phase} \times 100\% \quad (5)$$

where $\Delta Amplitude1$ and $\Delta Phase1$ are the amplitude relative errors and phase relative errors by the traditional FFT,

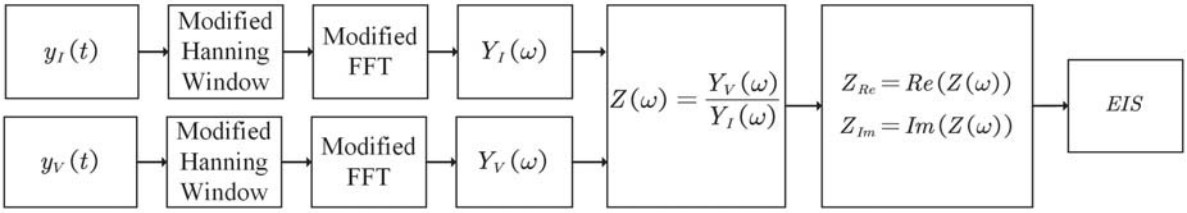

Figure 1. The principle of the Fast-EIS.

TABLE I. THE COMPARISON OF EXTRACTING RESULTS BETWEEN THE TRADITIONAL FFT AND THE FAST-EIS

	Frequency (Hz)	*Amplitude (V)*	*Phase (°)*	*Amplitude' (V)*	*Phase' (°)*	*Amplitude'' (V)*	*Phase'' (°)*
1	800	0.0300714	-1.91871	0.0301818	-1.90913	0.0302671	-1.91771
2	640	0.0301113	-2.3911	0.0303532	-2.40923	0.0301282	-2.39374
3	510	0.0301745	-2.98612	0.0302985	-3.00053	0.0301811	-2.98983
4	404	0.0302761	-3.74033	0.0302242	-3.76531	0.0302878	-3.74233
5	318	0.0304407	-4.69195	0.0306092	-4.65019	0.0304501	-4.69345
6	200	0.0310663	-7.10332	0.0309806	-7.12038	0.0310776	-7.10615
7	160	0.0316025	-8.50503	0.0314517	-8.52927	0.0316321	-8.49871
8	126	0.0324271	-10.0873	0.0323393	-10.1548	0.032413	-10.08445
9	100	0.0335244	-11.5554	0.0335535	-11.6078	0.0335417	-11.5656
10	80	0.0348791	-12.7372	0.0348274	-12.8141	0.0348536	-12.7413

respectively.

$$\Delta Amplitude2 = \frac{Amplitude^{"} - Amplitude}{Amplitude} \times 100\% \quad (6)$$

$$\Delta Phase2 = \frac{Phase^{"} - Phase}{Phase} \times 100\% \quad (7)$$

where $\Delta Amplitude2$ and $\Delta Phase2$ are the amplitude relative errors and phase relative errors by the Fast-EIS method, respectively. The box plots of the above four relative errors are shown in Fig. 2.

It can be seen that the Fast-EIS method improves the stability and accuracy of amplitude and phase extraction results compared to the traditional FFT method.

Fig. 3 illustrates a circuit model constructed by MATLAB. Two theoretical impedances can be obtained by two sets of circuit parameters which are shown in TABLE II. Setting the amplitude and phase of the theoretical current excitation signal in the frequency range 1Hz~10kHz, then the voltage response signal can be calculated by the model. Traditional FFT and the Fast-EIS method are separately used to extract the amplitude and phase results from the current and voltage signals in each frequency, Fig. 4 and Fig. 5 show the comparison EIS results of two tests.

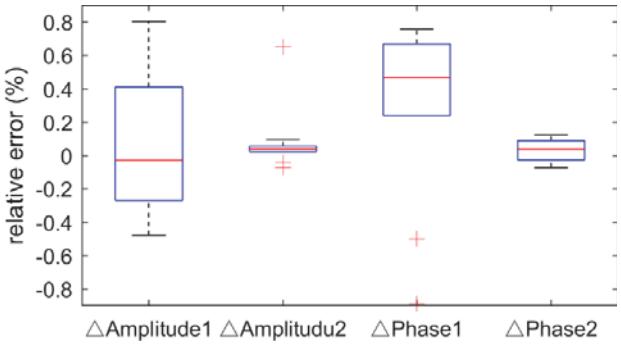

Figure 2. The relative errors of the extract results of the traditional FFT and the Fast-EIS

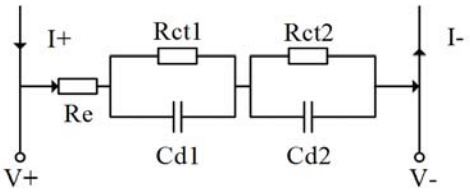

Figure 3. R(RC)(RC)circuit

In Fig. 4 and Fig. 5, the left diagrams are calculated by traditional FFT, and Fast-EIS calculate the right diagrams. The results extracted by Fast-EIS are much closer to theoretical values than the traditional FFT method. It makes the EIS curve smoother, and it has more benefits in analyzing the battery health state in further work.

III. HARDWARE IMPLEMENTATION AND VALIDATION

A. Hardware design

Fig. 6 shows the hardware modules and connection. The Data Acquisition Card (DAQ Card) is controlled by LabVIEW 2018 on PC. The resolution of the analog to digital converter (ADC) is 16 bits. When the measuring range is appropriate, the final resolution on the EIS complex plane is about $3\times10^{-5}\Omega$, it can meet the requirements of EIS analysis.

PC and the Fast-EIS measuring circuit connected by the SCSI-68P interface and a SHC68-68-EPM cable. The V-I converter circuit in the Fast-EIS measuring circuit can transform the voltage signal output by AO0 into a current signal, then input to the battery. The differential-acquisition channel AI1± collects the amplified and filtered voltage signal which is transformed from the current excitation by the current-sense resistor (RsNs). And AO1 is used to output a voltage signal equal to the OCV value of the battery, connected with the battery's negative electrode. The non-inverting input terminal of the differential operational amplifier is connected with the battery positive electrode, and the inverting input terminal is connected with AO1, then the DC voltage of the battery can be eliminated. AI0± collects the voltage response signal via the operational amplifier.

In this paper, the Fast-EIS measuring circuit is connected with the battery by a four-wire connector, two of them are used to input the current signal. The other two is used to measure voltage response. The four-wired connector can eliminate the wire resistance, while the three-wired connector used by the electrochemical workstations can only eliminate half of the wire resistance. This structure can improve the accuracy of the EIS measuring.

B. Hardware verification

The proposed hardware and a commercial electrochemical workstation (CHI660e, CHENHUA, Shanghai China) are used to measure the EIS of a 18650 type Lithium-ion battery (LR1865sk, LISHEN, Tianjin China) by sweep-frequency method, respectively. The comparison results are shown in Fig. 7, the blue line is from CHI660e, and the black line is from our

TABLE II. TEST PARAMETERS OF THE CIRCUIT MODEL

Test No.	*Re(Ω)*	*Rct1(Ω)*	*Cd1(μF)*	*Rct2(Ω)*	*Cd2(μF)*
1	0.06	0.03	22000	0.05	188000
2	0.03	0.015	220000	0.05	1880000

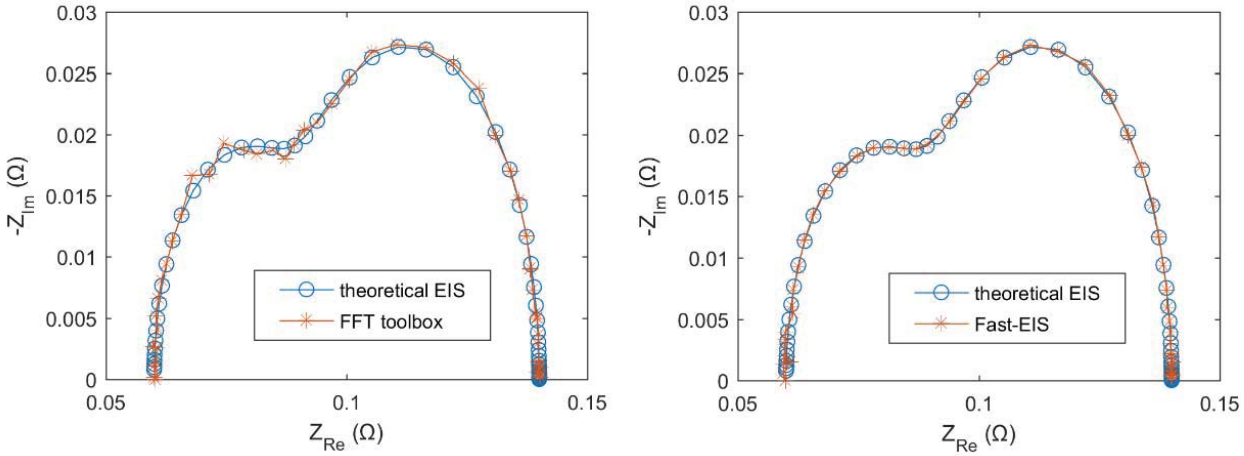

Figure 4. The comparison of the FFT toolbox and Fast-EIS results for Test 1.

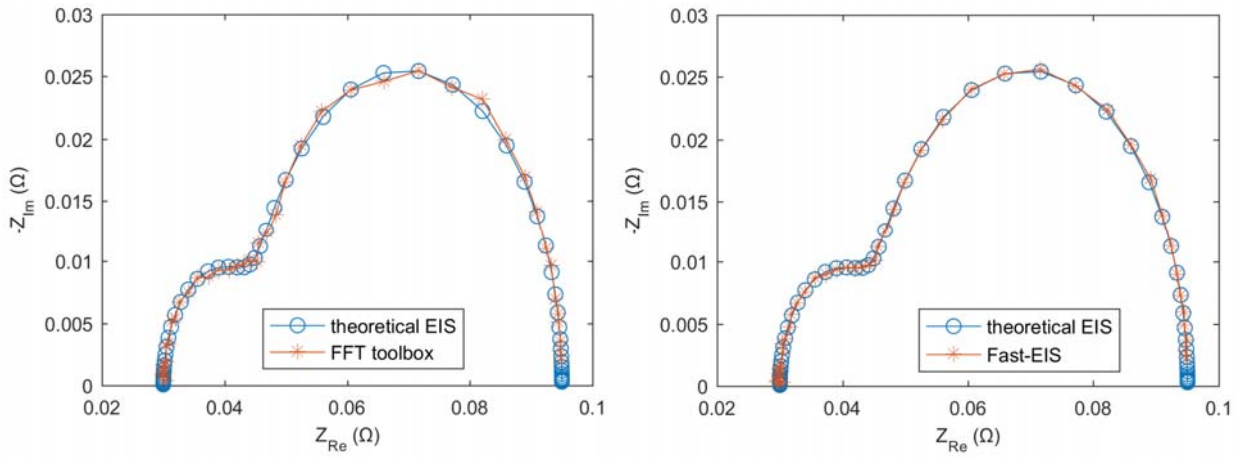

Figure 5. The comparison of the FFT toolbox and Fast-EIS results for Test 2.

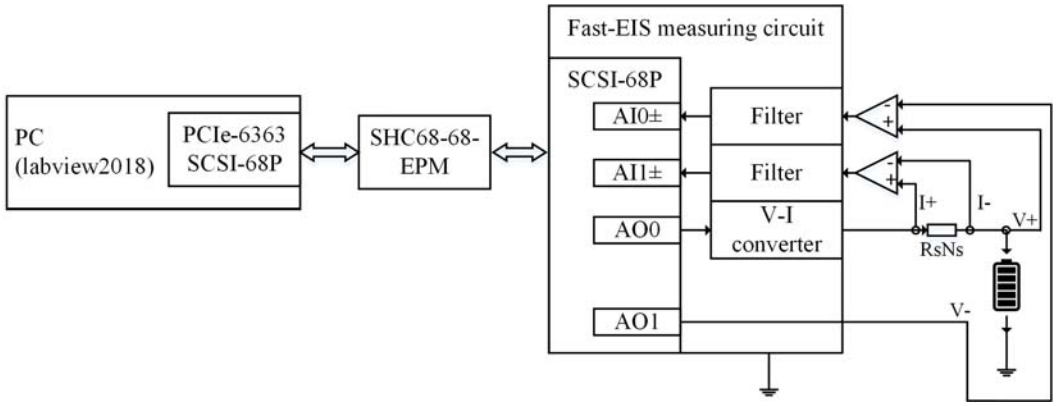

Figure 6. Hardware design

hardware.

The measuring EIS curves on the complex plane have an obvious shift. The reason is that the electrochemical workstation has wire resistance because it used a three-wired connector. To verify this phenomenon, a four-wired battery internal resistance measuring instrument (CR-20V-2000mΩ, NEWARE, Shenzhen China) is used to measure the internal resistance of the battery at 1kHz. The result is very the same with the proposed method, so it can be confirmed that the wire resistance is 163mΩ, and causes the shift.

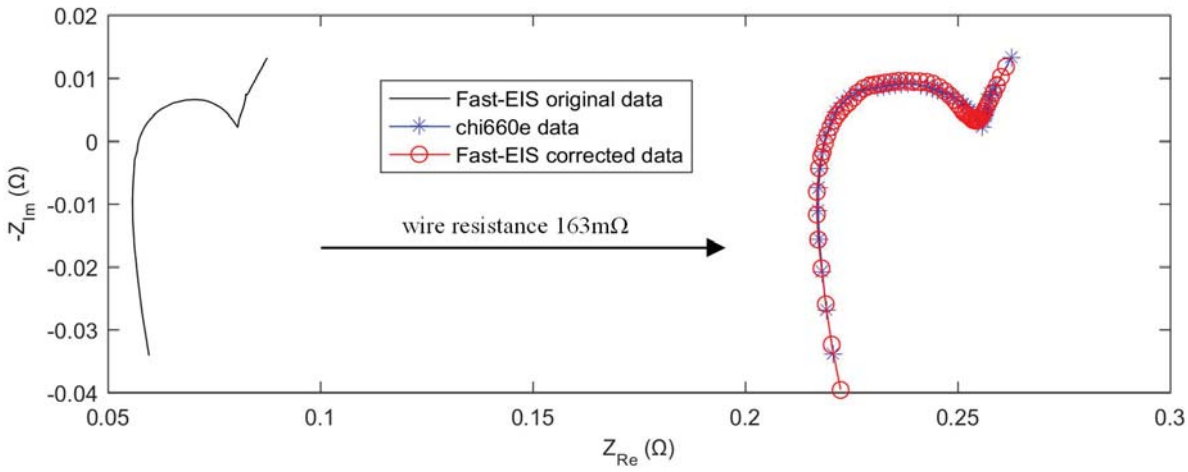

Figure 7. Comparison of the EIS curves from CHI660e and the purposed hardware.

There are still some differences between the two curves after shifting. The season is the parasitic capacitance and parasitic resistance [10] caused by the connector between the electrochemical workstation and battery, which composed by an aviation plug and alligator clips. These differences reflected on the equivalent circuit model are approximately 0.4F and 10mΩ. The final EIS curve can be obtained by correcting via this equivalent circuit model, shown by the red line in Fig. 7.

IV. FAST-EIS RESULTS OF REAL BATTERIES

Other two LR1865sk batteries are used for EIS measuring, and the corrected method mentioned above is used to obtain the final curves. Fig. 8 shows the Fast-EIS result compared with the CHI660e data of a fresh battery No. SK01. And Fig. 9 shows the results of an aged battery No. SK20.

The EIS results of Fast-EIS method are almost the same as those of electrochemical workstation. It proves that the Fast-EIS measuring circuit and the Fast-EIS algorithm are feasible. The measuring time of the proposed method is 580s, reduces 2/3 time compared with the electrochemical workstation. It is more suitable for practical application in engineering.

V. CONCLUSION

This paper proposes a Fast-EIS measuring method, which can reduce 2/3 time compared with a commercial electrochemical workstation. The measurable frequency range is 0.01Hz to 10kHz, and it meets the requirements for EIS analysis. The verification experiment shows that the proposed method has almost the same accuracy with the existing instruments, and the four-wired connector can effectively eliminate the wire resistance, make the EIS results more credible. The hardware is easy to implement, and the method is more suitable for practical application in engineering.

In the future, this proposed method will be used for multi-batteries measuring. Due to the shortened measurement time, the EIS results will be more accurate, because the battery state changes by excessive measuring time are avoided. What's more, an 8-channel automatic EIS instrument is under designed using the proposed method, which can provide experimental support for researching the energy storage battery of marine energy power station.

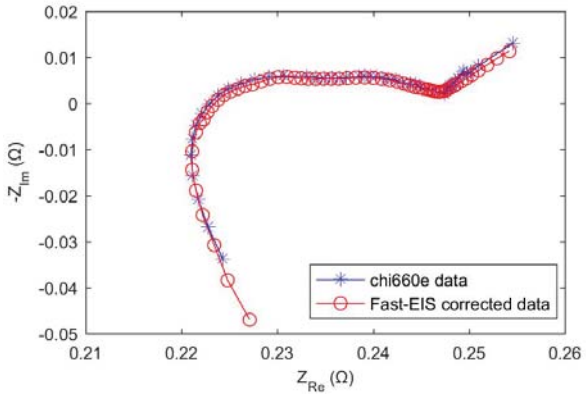

Figure 8. Comparison of the EIS curves from CHI660e and the purposed method for No. SK01.

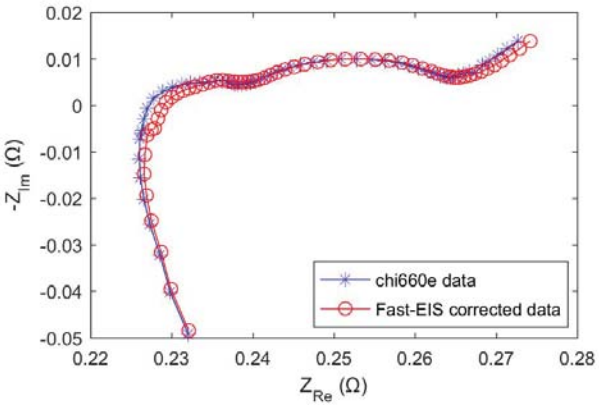

Figure 9. Comparison of the EIS curves from CHI660e and the purposed method for No. SK20.

ACKNOWLEDGMENT

This research was financially supported by the National Natural Science Foundation of China (NSFC Grant 51607167 and 51761135014). We are also grateful to all anonymous reviewers for providing useful comments and suggestions that resulted in the improved quality of this paper.

REFERENCES

[1] L.Q. Zhang, L. J. Liu, R. Yang, K. Wang, Z. Chen and M. Li, "A roadmap for modeling and feature extraction of energy storage battery pack for marine energy power station," in Prognostics and System Health Management Conference , Harbin, 2017, pp. 1032-1038.

[2] H.Wang and L. Guo, "Applications of electrochemical impedance spectroscopy in detection of lithium battery state," Chinese Journal of Power Sources, vol. 38, pp. 73-74, 2014.

[3] T. Stanciu , D. I. Stroe, R. Teodorescu, and M.Swierczynski,"Extensive EIS characterization of commercially available lithium polymer battery cell for performance modelling," in European Conference on Power Electronics and Applications New York: IEEE, 2015.

[4] C. Pastor-Fernandez , W. Dhammika Widanage , J. Marco , M. Gama-Valdez , G. H. Chouchelamane, "Identification and quantification of ageing mechanisms in Lithium-ion batteries using the EIS technique," in 2016 IEEE Transportation Electrification Conference and Expo(ITEC), 2016, pp. 1-6.

[5] F. Cheng, "Study on performance of lithium ion battery still placed," Physics Examination and Testing, vol. 27, pp. 27-30, 2009.

[6] K. R. Rao, D. N. Kim and J. J. Hwang, "Fast fourier transform - Algorithms and Applications," 2010.

[7] D. Megias, J. Serra-Ruiz and M. Fallahpour, "Efficient self-synchronised blind audio watermarking system based on time domain and FFT amplitude modification," Signal Processing,vol. 90,pp.3078-3092, 2010.

[8] A. Boughambouz, A. Bellabas, B. Magaz, T. Menni, and M. E. Abdel Aziz, "Improvement of radar signal phase extraction using all phase FFT spectrum analysis," New York: IEEE, 2017.

[9] B. Zeng, Z. Teng, Y. Cai, S. Guo, and B. Qing, "Harmonic phasor analysis based on improved FFT algorithm," IEEE Transactions On Smart Grid, vol. 2, pp. 51-59, 2011.

[10] Y. Xie, J. Li and C. Yuan, "Mathematical modeling of the electrochemical impedance spectroscopy in lithium ion battery cycling," Electrochimica Acta, vol. 127, pp. 266-275, 2014.